3D PRINTING OF A BIOCOMPATIBLE SCAFFOLD AND A REAL-TIME IMAGING WINDOW FOR MONITORING RAT SPINAL CORD REGENERATION

A THESIS SUBMITTED TO THE FACULTY OF UNIVERSITY OF

MINNESOTA BY

MIHIR A. MADHAPARIA

IN PARTIAL FULFILLMENT FOR THE REQUIREMENTS FOR THE

DEGREE OF MASTER OF SCIENCE

ADVISORS: DR. MICHAEL C. McALPINE, DR. ANN M. PARR

JANUARY 2026

Acknowledgements

Throughout the course of this thesis, many individuals and specific laboratories have helped me grow through their mentorship, shared knowledge, and practical experience.

First and foremost, I would like to express my deepest gratitude to my family for their constant encouragement, patience, and unwavering support throughout my educational journey. Their belief in me made this work possible.

I would like to also express my sincere gratitude to my advisors, Dr. Michael C. McAlpine and Dr. Ann M. Parr, for their continued support, critical insight, and guidance throughout the duration of my masters thesis. Their mentorship has been instrumental in shaping my understanding of 3D printing and neural tissue.

Next, I thank my examining committee: Dr. Suhasa Kodandaramaiah and Dr. Nichole Morris, for the time, effort, and valuable insight they provided during the review of my thesis and defense.

Additionally, I would like to thank my fellow lab mates in the McAlpine Research Group for their valuable discussions and willingness to offer insight when challenges arose, with special thanks to Hyunjun Kim for his camaraderie and technical support. I am also grateful to the members of the Parr Research Group for their continued support and guidance.

Finally, I would like to thank Paul Rothweiler and the Bakken Medical Device Center for providing access to 3D printing and prototyping facilities.

Abstract

The development of effective regenerative therapies for spinal cord injury (SCI) remains limited by two critical challenges: the absence of structurally optimized bridging scaffolds and the inability to monitor biological integration in real time. Conventional experimental approaches rely primarily on endpoint histological analysis, offering limited insight into the dynamic cellular processes underlying repair or failure. This thesis addresses these challenges through a dual-objective framework involving the fabrication of a biocompatible, 3D-printed neural scaffold and the development of a chronic spinal imaging window for longitudinal in vivo visualization. Candidate scaffold materials- polycaprolactone (PCL), poly(lactic-co-glycolic acid) (PLGA), and silicone- were evaluated to balance mechanical compliance with biological performance. While PLGA exhibited favorable mechanical characteristics, PCL demonstrated superior cytocompatibility, cellular attachment, and handling robustness. By integrating a regenerative scaffold with a platform for real-time monitoring, this work establishes an analytical framework to reduce translational risk and advance implant-based SCI therapies.

Table of Content

Chapter 1: Introduction

This chapter establishes the critical context and motivation for the research presented in this thesis. It begins by outlining the profound clinical, social, and economic burden of spinal cord injury (SCI), thereby defining the unmet need for effective regenerative therapies. It proceeds to critically evaluate the current therapeutic landscape, identifying key limitations- specifically the "black box" of in vivo monitoring- that impedes progress. A comprehensive literature review of emerging technologies in 3D bioprinting is then presented, utilizing recent comparative literature to weigh the trade-offs between resolution, biocompatibility, and mechanical integrity. Finally, the specific objectives of this thesis are articulated, followed by a structural overview of the subsequent chapters.

1.1 The Unmet Clinical Need in Spinal Cord Injury

Spinal cord injury (SCI) represents a devastating and life-altering neurological condition with profound consequences for individuals, families, and society at large. Globally, over 15 million people are living with SCI, a condition that results in long-term disability and accounts for over 4.5 million years of life lived with disability (YLDs) annually.[1] In the United States, the scale of the problem is similarly stark, with an estimated annual incidence of 54 cases per million people, translating to approximately 18,000 new injuries each year.[2] The total number of individuals living with SCI in the U.S. is estimated to be around 302,000.[2] The majority of these injuries are traumatic in nature, with motor vehicle accidents and falls being the leading causes, resulting in acute physical damage to the delicate neural tissue of the spinal cord.[1]

Beyond the immediate physical trauma, SCI imposes a staggering and lifelong economic burden. Individuals living with paralysis face significant financial hardship, with approximately 28% of affected households earning less than $15,000 per year.[2] Employment rates are drastically reduced, with only 15.5% of individuals with paralysis employed compared to 63.1% of the non-disabled population.[2] The direct lifetime costs of care are immense, ranging from over $1.8 million for individuals with preserved motor function to more than $5.4 million for those with high tetraplegia.[3] These figures do not account for indirect costs such as lost wages and productivity, which often exceed the direct medical expenses.[1]

Compounding this challenge is a critical demographic shift. The average age at the time of injury has increased significantly, from 29 years in the 1970s to 44 years since 2015.[3] This trend has profound socio-economic implications. An injury sustained at age 44 occurs during a person's peak earning years, disrupting established careers and severely impacting family finances and societal economic productivity. This demographic reality transforms the quest for a cure from a purely medical goal into a pressing economic imperative. The current paradigm of lifelong supportive care is not only financially unsustainable but also fails to restore the individual's functional independence and quality of life. Consequently, there is an urgent and compelling need for a paradigm shift away from palliative management and toward a curative, regenerative solution that can restore neurological function, return individuals to the workforce, and alleviate the immense long-term economic drain on public and private resources.

1.2 Pathophysiology of Spinal Cord Injury: The Biological Barrier

To engineer effective therapeutic scaffolds, one must first dissect the hostile biological environment they are intended to bridge. The pathophysiology of SCI is a dynamic, multi-phasic process where the initial trauma sets off a self-propagating wave of tissue destruction.

1.2.1 The Primary and Secondary Injury Cascades

The injury process is temporally divided into the primary and secondary injury phases. The primary injury is the immediate mechanical disruption- contusion, compression, or transection- that shears axons and ruptures blood vessels. This is followed almost immediately by the secondary injury, a cascade of deleterious biochemical events that expand the lesion size and exacerbates functional loss.

- Acute Phase (<48 Hours): Vascular disruption leads to ischemia and hemorrhage. The breakdown of the Blood-Spinal Cord Barrier (BSCB) allows the infiltration of neutrophils and macrophages, triggering an inflammatory storm.5 Ionic imbalance, specifically the influx of intracellular calcium (Ca 2+), triggers excitotoxicity and the release of reactive oxygen species (ROS), leading to widespread neuronal necrosis.[6]
- Subacute Phase (2 Days – 2 Weeks): This phase is characterized by the proliferation of reactive astrocytes. While these cells attempt to contain the injury, they begin to form the glial scar-dense, physical barrier rich in Chondroitin Sulfate Proteoglycans (CSPGs) that chemically inhibits axonal regeneration.[6]
- Chronic Phase (>6 Months): The lesion site stabilizes into a cystic cavity surrounded by a

dense glial scar.[3] This cystic gap acts as a physical chasm that regenerating axons cannot cross without a bridging substrate.

1.3 A Critical Review of Current Therapeutic Landscapes

Despite significant advances in our understanding of SCI pathophysiology, clinical management remains supportive rather than curative.

1.3.1 Surgical Decompression

The current standard of care for acute spinal cord injury is predicated on the mitigation of secondary injury mechanisms through early surgical decompression and hemodynamic stabilization. Following the primary mechanical impact, the spinal cord undergoes a rapid and devastating cascade of secondary events, including gross edema, hemorrhage, and vasospasm. These processes collectively increase intraspinal pressure, compressing the microvasculature and inducing critical ischemia in the surviving neural tissue surrounding the lesion core.

The clinical imperative to address this pathology is encapsulated in the "Time is Spine" concept, which advocates for surgical intervention within the first 24 hours of injury. The objective is to physically relieve osseous or ligamentous pressure on the cord, thereby restoring capillary perfusion and limiting the extent of secondary ischemic necrosis. This approach was rigorously validated by the landmark Surgical Timing in Acute Spinal Cord Injury Study (STASCIS), a multi-center prospective cohort study led by Fehlings et al. (2012).[4]

The STASCIS trial compared the outcomes of patients undergoing early decompression (<24 hours post-injury) versus those receiving delayed treatment (>24 hours). The study reported that patients in the early surgical cohort were 2.8 times more likely to achieve a significant neurological recovery, defined as an improvement of at least two grades on the ASIA Impairment Scale (AIS) at the six-month follow-up, compared to the delayed group.[4] By statistically confirming the window of therapeutic opportunity, STASCIS established early decompression as the global gold standard for acute management.

However, while early decompression significantly improves the probability of functional recovery, it remains a strictly neuroprotective intervention rather than a regenerative one. Its primary function is to salvage the "penumbra"- the threatened but viable tissue at the periphery of the injury- rather than to repair the damage already sustained. Even with successful early intervention, the fundamental architecture of the spinal cord remains disrupted; decompression cannot bridge the physical gap created by the lesion, nor can it induce the regrowth of severed axons across the inhibitory glial scar. Consequently, while surgical stabilization is a necessary prerequisite for recovery, it fails to address the underlying biological need for structural repair, highlighting the critical necessity for bio-engineered scaffolds that can actively promote regeneration.

1.3.2 Pharmacological Interventions

Pharmacological strategies have been investigated with limited success.

- Corticosteroids: The historical use of high-dose methylprednisolone (MPSS) to reduce inflammation is now highly controversial. Recent guidelines indicate that the risk of severe adverse events, including gastrointestinal hemorrhage and wound infection- often outweighs the modest motor benefits.[11]
- Emerging Agents: Riluzole, a sodium channel blocker, has shown promise in preclinical models by reducing excitotoxicity, though clinical translation remains ongoing.

1.3.3 Rehabilitation

In the absence of curative biological therapy, physical rehabilitation remains the only therapeutic intervention with proven clinical efficacy in enhancing functional independence following spinal cord injury. Unlike surgical decompression, which is a passive neuroprotective measure, rehabilitation actively engages the neuromuscular system to drive functional recovery through the mechanism of activity-dependent neuroplasticity. This process involves the reorganization of neural pathways and the strengthening of synaptic connections in response to repetitive physiological stimuli.[5]

Modern rehabilitation strategies, particularly Body-Weight Supported Treadmill Training (BWSTT), have shifted focus from simply teaching compensatory maneuvers to activating intrinsic spinal circuitry. Research has demonstrated that the mammalian spinal cord possesses autonomous neural networks known as Central Pattern Generators (CPGs). These local circuits are capable of generating rhythmic motor outputs, such as stepping, even in the absence of supraspinal input from the brain.[6] As demonstrated in seminal work by Behrman and Harkema

(2000), providing intense, task-specific sensory cues- such as loading the limbs and extending the hips during treadmill walking- can "wake up" these dormant CPGs.[5] This training promotes the sprouting of spared axons and the remodeling of local synaptic connections, allowing patients with incomplete injuries to significantly improve walking ability and standing tolerance.

However, while neuroplasticity offers a powerful avenue for improvement, it is fundamentally limited by the underlying anatomy. As noted by Dietz (2008) in a critical review of spinal locomotion, the success of rehabilitation is strictly contingent upon the presence of spared neural tissue.[7] Rehabilitation can optimize the function of surviving pathways, but it cannot induce the de novo regeneration of severed axons across the lesion site. It cannot bridge the physical gap created by the glial scar, nor can it reconnect long-distance tract systems that have been completely transected. Consequently, rehabilitation eventually reaches a therapeutic plateau- a "glass ceiling" determined by the severity of the initial trauma. To break through this ceiling and restore function in severe or complete injuries, rehabilitation must be paired with a regenerative substrate- such as a bio-printed scaffold- that can physically bridge the injury gap and provide new real estate for axonal growth.

1.3.4 Foundational Advances in Scaffold Design: From Architecture to Nano-Functionality

The transition from simple porous blocks to anatomically relevant neural interfaces has been driven by pivotal research demonstrating that scaffold architecture is as critical as material chemistry. Several pioneering research groups have established foundational principles that guide modern spinal scaffold design, moving beyond simple mechanical support to creating

sophisticated, multi-scale environments that actively direct regeneration.

A seminal advancement in the integration of living biological components with synthetic architecture was demonstrated by the McAlpine Research Group at the University of Minnesota. In their landmark 2018 study (Joung et al., Advanced Functional Materials), the group tackled the historical challenge of cell viability in extrusion printing. Traditional methods often required seeding cells onto a prefabricated scaffold, resulting in poor infiltration and non-uniform distribution.[8]

To overcome this, McAlpine's team developed a novel multi-material 3D bioprinting platform. As illustrated in Figure 1, this system utilized a precise, layer-by-layer deposition strategy to print neural progenitor cells (NPCs) encapsulated within a hydrogel bio-ink simultaneously with a silicone-based supporting matrix. This "one-pot" fabrication method allowed for the creation of continuous "axonal guidance channels" fully populated with living cells throughout the scaffold's volume. Their results demonstrated that these printed channels could successfully orient the growth of differentiating neurons, effectively forcing axons to propagate in a linear, organized fascicle rather than a random tangle. This work established the critical baseline that printed geometry- specifically continuous micro-channels can physically dictate the directionality of neural repair.

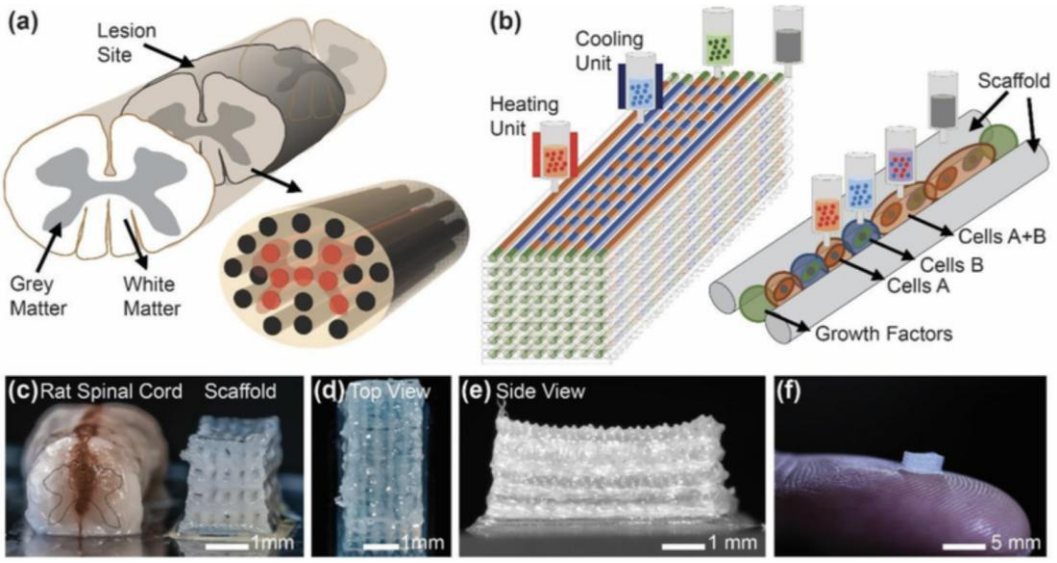

Figure 1: Experimental strategies for 3D bioprinting spinal cord tissue. (a) Schematic of the spinal cord illustrating grey matter and white matter boundaries and a design for a 3D bioprinted multichannel scaffold for modeling the spinal cord. (b) Schematic overview of the 3D bioprinting process. Biocompatible bioinks are extruded at specific temperatures (37 °C or 4 °C, depending on the bioink) in a layer-by-layer process. The scaffold ink is structurally supportive and can be made with a biocompatible material. (c) Comparison of a transected rat spinal cord and the design principle for scaffolds consisting of multiple, continuous channels. The number of channels can be scaled according to the size of the scaffold needed. (d) Top view image of scaffold channels demonstrates a printing resolution of ~150 μm. Channels are continuous throughout the scaffold, allowing for axonal extension. (e) Side view of a 5 mm long scaffold. (f) A 2×2×5 mm3 sized scaffold on top of a finger shows the scale of a scaffold. Adapted from Joung et al. (2018) [8].

Complementing the manufacturing innovations of the McAlpine group, the Tuszynski lab at UCSD (Koffler et al., Nature Medicine, 2019)[9] addressed the challenge of "anatomical fit." Spinal cord injuries are rarely uniform; they present as irregular, cystic cavities. Generic cylindrical scaffolds often fail to integrate because they do not match the complex geometry of the lesion, leading to gaps where scar tissue can form.[9]

Using rapid 3D bioprinting of polyethylene glycol (PEG) hydrogels, Tuszynski's team developed a "scan-to-print" workflow. They utilized MRI scans of the host spinal cord to generate a digital model of the lesion site, which was then used to print a custom scaffold that perfectly matched the injury geometry. Their findings, depicted in Figure 2, revealed that scaffolds containing linear micro-channels (200µm diameter) aligned with the host white matter supported robust axonal regeneration. However, they also noted a critical mechanical trade-off: while soft hydrogels are biocompatible, they often lack the long-term structural integrity to withstand the compressive forces of the spinal column, leading to potential collapse. This limitation underscores the objective of this thesis: to adopt the channel architecture validated by Tuszynski but fabricate it using structurally robust thermoplastics (PCL/PLGA).

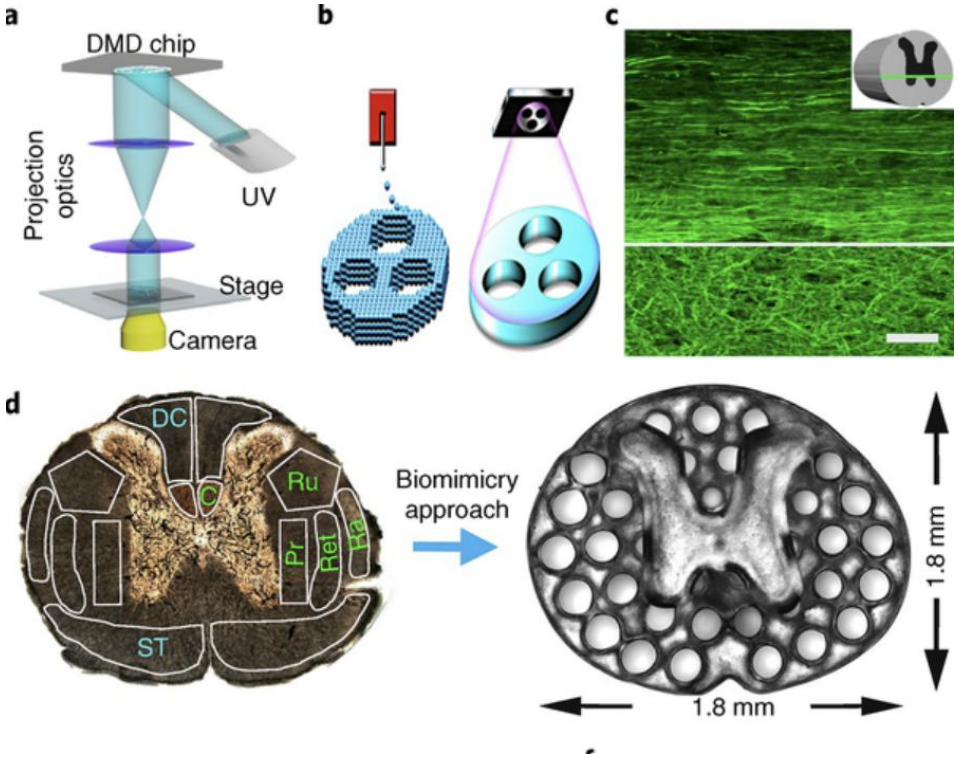

Figure 2: Biomimetic scaffold design workflow. (A) MRI scan of the spinal cord is segmented to create a lesion-specific digital model. (B) The printed scaffold featuring circular micro-channels designed to bridge the injury gap. (C) In vivo result showing axons (green) regenerating through the printed channels, bridging the lesion. (D) 3D printed scaffolds developed based on information collected about neuronal exchange in varying cross-sections of the spinal cord. Adapted from Koffler et al. (2019) [9].

While architecture guides direction, the surface of the scaffold dictates cellular adhesion and signaling. The Zhang Research Group at George Washington University has pioneered the integration of nanomaterials into 3D printed neural scaffolds to mimic the hierarchical structure

of the extracellular matrix (ECM). In their work (Lee et al., 2018), they recognized that standard 3D printed filaments (like PCL) are biologically inert and electrically insulate a significant drawback for conductive neural tissue.[10]

To address this, the Zhang group developed stereolithography-based scaffolds incorporating multi-walled carbon nanotubes (MWCNTs) and tunable nano-roughness. As shown in Figure 3, these "smart" scaffolds provide dual cues: the 3D printed micro-channels provide gross guidance, while the nanomaterials provide electrical conductivity and nano-scale roughness that enhances neurite extension. Their research demonstrated that neural stem cells cultured on these conductive, nano-enhanced scaffolds exhibited significantly higher proliferation and differentiation rates compared to smooth polymer controls, specifically in the neurite lengths of NSCs. This highlights a crucial evolution in the field: 3D printing is no longer just about shaping plastic; it is about creating a bioactive, conductive chassis that actively stimulates regeneration.

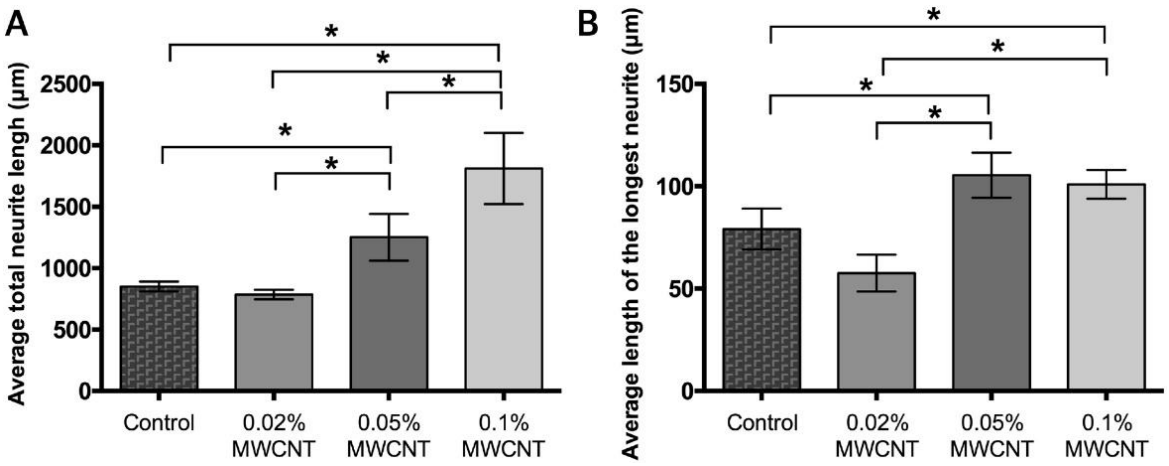

Figure 3: Quantification of neurite length of NSCs on 3D printed scaffolds with or without MWCNTs after 8 d of culture. Neurite length was analyzed using ImageJ software and NeuriteTracer. (A) Total neurite length. (B) Average length of the longest neurite per cell. Data are mean ± standard error of the mean, n = 6, *p < 0.05 when compared to corresponding groups at day 8. Adapted from Lee et al. (2018) [10].

1.3.5 Recent Advances: From Static Support to Dynamic Immunomodulation

The field of spinal cord regeneration is rapidly evolving from the design of static, structural bridges to the development of dynamic, "smart" scaffolds that actively manipulate the injury microenvironment. While early work focused primarily on guiding axons, research published in recent years has demonstrated that successful regeneration requires addressing the complex immune response and the dynamic mechanical environment of the spinal cord. Three key areas of innovation have emerged: conductive hydrogel integration, immunomodulatory surface engineering, and injectable/shape-conforming designs.

Recent work has moved beyond simple conductive coatings to fully integrated conductive hydrogels. Leahy et al. (2024) developed a 3D printed scaffold incorporating conductive Pedot:PSS polymers that not only guided axons but actively stimulated myelination through electrical cues. Their work showed that electrical conductivity is not just for signaling but is a critical factor in the maturation of regenerated nerve fibers, significantly enhancing the thickness of the myelin sheath compared to non-conductive controls.[11]

Stiffness-Mediated Immunomodulation Perhaps the most significant paradigm shift in recent years is the discovery that the immune response to a scaffold is governed not only by surface chemistry but fundamentally by mechanical stiffness. In a 2025 breakthrough study, Ye et al. demonstrated that 3D-printed PLGA scaffolds could modulate the immune microenvironment purely through the tuning of their mechanical properties, without the need for exogenous anti-inflammatory drugs.[12] By fabricating PLGA scaffolds with varying stiffness profiles, the researchers identified a mechanism of "mechanical immunomodulation." They observed that scaffolds matching the low modulus of native spinal cord tissue significantly inhibited the activation of pro-inflammatory (M1) macrophages and foreign body giant cells. This is shown on figure 4 below. Conversely, stiffer scaffolds triggered a severe inflammatory response. The "soft" PLGA scaffolds naturally promoted a transition toward the regenerative (M2) macrophage phenotype (CD206+), resulting in a reduced glial scar and enhanced axonal regrowth. This finding is critical as it suggests that the material "softening" observed in printed PLGA may inherently confer an immunological advantage over rigid polymers like PCL.

Injectable and Shape-Conforming Scaffolds To solve the problem of surgical

invasiveness, Tigner et al. (2024) pioneered the use of "injectable" 3D printed granular hydrogels. Figure 5 below shows an animated diagram of the granulated hydrogel injected on the spinal cord as well as the GFP imaging done to show the live/dead assays of implanted cells as various time points. Unlike rigid PCL blocks that require open surgery, these scaffolds are printed as micro-scale porous granules that can be injected through a needle. Once in the lesion cavity, they self-assemble into a porous scaffold that perfectly fills the irregular cystic defect, solving the "mechanical mismatch" problem entirely by conforming to the host tissue geometry.[13]

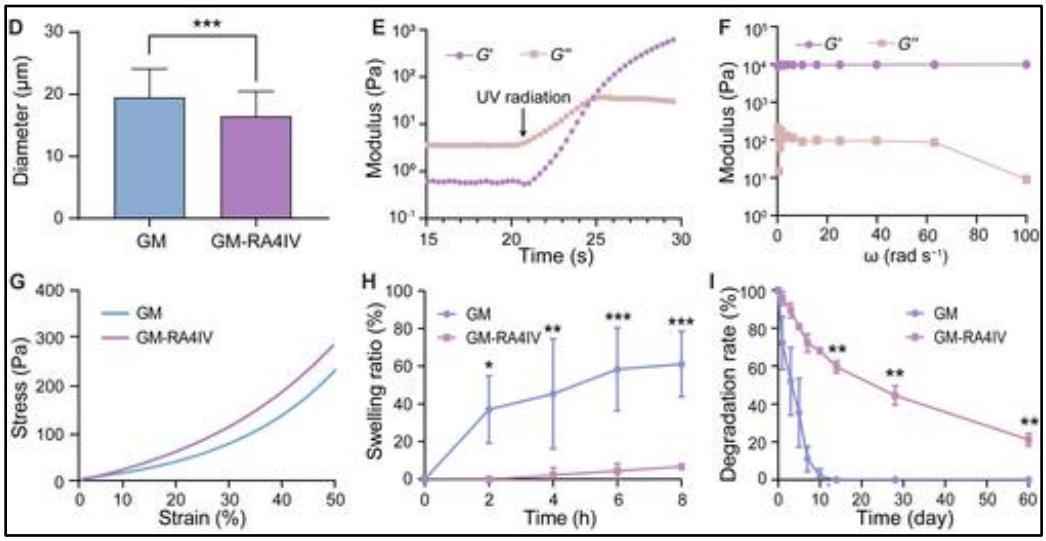

Figure 4: Stiffness-mediated immunomodulation. Evidence that matching the mechanical compliance of the scaffold to the native tissue naturally resolves inflammation. Fluorescence microscopy reveals that softer 3D-printed PLGA scaffolds (right) promote the infiltration of regenerative M2 macrophages (CD206+, green) and suppress pro-inflammatory M1 markers

(CCR7+, red) compared to stiffer scaffolds, which elicit a foreign body response. Adapted from Ye et al. (2025) [12]

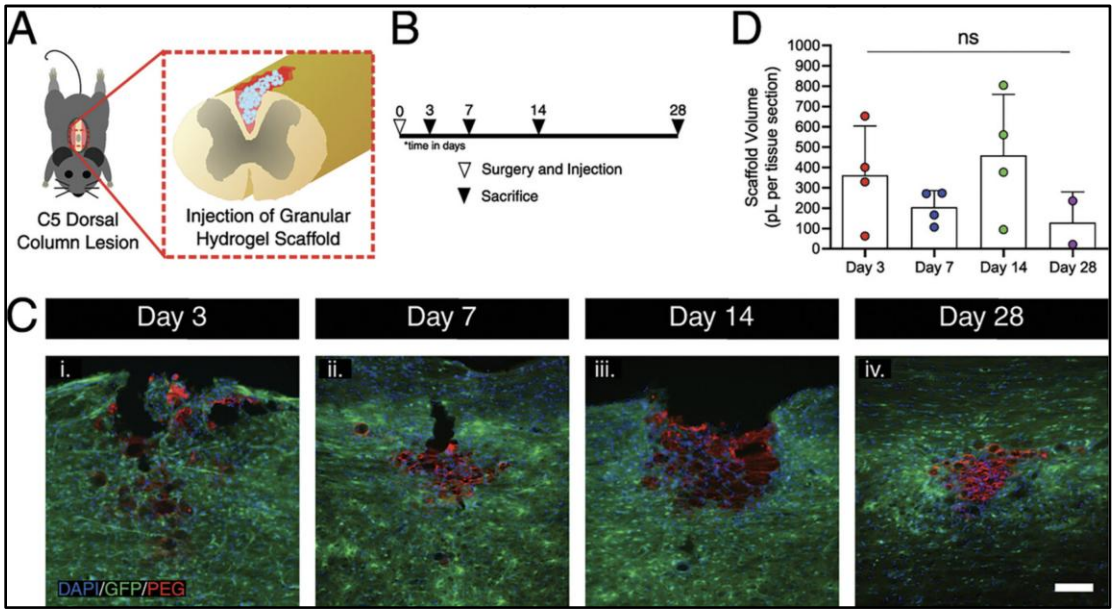

Figure 5: Minimally invasive deployment via granular hydrogels. Illustration of the "injectable scaffold" concept. Unlike pre-formed rigid scaffolds that require invasive surgical implantation, 3D-printed granular hydrogels can be injected directly into the lesion site via a syringe. The granular nature allows the scaffold to flow and conform perfectly to the irregular, cystic topography of the injury (right), eliminating void spaces and ensuring seamless tissue-material integration. Adapted from Tigner et al. (2024) [13]

1.4 Emerging Frontiers in SCI Repair: 3D Bioprinting as a Paradigm Shift

The limitation of current therapies necessitates a tissue engineering approach. 3D bioprinting offers a transformative solution by enabling the fabrication of "bridge" scaffolds that

physically and chemically guide regenerating axons across the lesion site. Unlike random porous sponges created by salt-leaching, 3D printing provides deterministic control over micro-architecture, allowing for the creation of linear channels that mimic the fascicular organization of the spinal cord.[15]

1.4.1 Comparative Evaluation of Printing Modalities

The selection of the printing modality is critical, involving trade-offs between resolution, material compatibility, cell viability, and fabrication speed. A recent comprehensive review published in the International Journal of Extreme Manufacturing provides a pivotal comparison of these technologies.[14]

1.4.1.1 Extrusion-Based Bioprinting (EBB)

Extrusion-based bioprinting is currently the most widely utilized modality for fabricating macroscopic tissue constructs. This technique functions by dispensing continuous filaments of material- either a molten thermoplastic or a cell-laden hydrogel, through a micro-nozzle using pneumatic pressure or mechanical (piston or screw) force.

The primary advantage of EBB is its exceptional material versatility. It is the only modality capable of processing high-viscosity synthetic polymers (such as PCL and PLGA) necessary for structural support, as well as high-density cell slurries that mimic native tissue cellularity. By depositing material layer-by-layer, EBB can generate clinically relevant

volumetric constructs (cm-scale) with reasonable speed.

The critical drawback of EBB is the shear stress generated at the nozzle wall. As the bioink is forced through a narrow orifice (typically 100–400 μm), cells experience significant shear forces that can rupture cell membranes. Studies indicate that cell viability in EBB typically ranges from 40% to 80%, decreasing as nozzle pressure increases and nozzle diameter decreases. Furthermore, the resolution is limited by the die-swell phenomenon, where the extruded filament expands upon exiting the nozzle, limiting feature sizes to approximately 100–200 μm.

1.4.1.2 Inkjet-Based Bioprinting

Adapted from standard desktop printing technology, inkjet bioprinting operates by ejecting discrete droplets of liquid bioink onto a substrate. These droplets are generated either by a thermal actuator (which creates a vapor bubble to force ink out) or a piezoelectric actuator (which mechanically pulses the fluid).

Inkjet printing offers superior speed and cost-effectiveness. Because the droplets are extremely small (picoliter volume), this method allows for high-resolution patterning (~50 μm) and precise control over the placement of individual cells or growth factors. Cell viability is generally high (>85%) because the cells are not subjected to the sustained shear stress found in extrusion.

The major limitation of inkjet printing is the stringent requirement for low viscosity. To prevent nozzle clogging, bioinks must be in a liquid state (<15 mPas) during printing. This

makes it extremely difficult to stack layers vertically to create structurally rigid 3D scaffolds suitable for spinal cord implantation; the liquid droplets tend to spread and fuse, losing shape fidelity before they can crosslink. Consequently, inkjet printing is better suited for surface patterning rather than building volumetric bridges.

1.4.1.3 Stereolithography (SLA) and Digital Light Processing (DLP)

Light-assisted bioprinting techniques, such as SLA and DLP, utilize photosensitive bioinks that solidify (polymerize) upon exposure to light. SLA uses a laser beam to trace a pattern point-by-point, while DLP projects an entire image of a layer simultaneously using a digital micro-mirror device.

These methods offer the highest resolution among macroscopic printing techniques, capable of fabricating complex, overhang geometries with feature sizes <50 μm. The absence of a nozzle eliminates shear stress, theoretically improving cell viability during the printing process itself. The resulting scaffolds have smooth surfaces and high structural fidelity.

The primary concern in neural applications is cytotoxicity. The photopolymerization process requires photo-initiators (e.g., Irgacure 2959) which generate free radicals. These radicals, along with UV light exposure, can cause DNA damage to sensitive neural stem cells. While newer, visible-light initiators like LAP (Lithium phenyl-2,4,6-trimethylbenzoylphosphinate) are reducing this risk, the choice of materials is restricted to photocurable polymers, limiting the use of standard FDA-approved thermoplastics like PCL.

1.4.1.4 Melt Electrowriting (MEW)

Melt electrowriting is a hybrid technology that combines the principles of melt extrusion and electrospinning. A high-voltage electric field is applied between the nozzle and the collector, which draws the molten polymer filament into an ultra-fine jet.[14]

Unlike traditional electrospinning which produces random non-woven mats, MEW allows for the precise, computer-controlled deposition of aligned fibers with diameters in the range of 2–50 μm. This scale closely mimics the dimensions of axons and extracellular matrix fibers. For SCI repair, MEW is uniquely capable of creating highly anisotropic scaffolds that can physically guide regenerating axons in a straight line.

MEW is technically complex and slow. The deposition rate is significantly lower than extrusion or SLA, making it impractical for fabricating large, solid blocks of tissue. Furthermore, the high voltage and temperature required to melt the polymer preclude the direct incorporation of cells during the printing process; cells must be seeded onto the scaffold post-fabrication.

Table 1 below synthesizes the comparative analysis of 3D printing techniques specifically for nerve regeneration applications.

Table 1: Comparative evaluation of 3D printing technologies for neural tissue engineering. Adapted from Song et al., "Advances in 3D printing scaffolds for peripheral nerve and spinal cord injury repair".

Technology	Advantages	Disadvantages
Inkjet printing	• Simple method • High resolution • High accuracy • High cell viability • Applicability of multi-material printing	• Limited to cell density • Limited to viscosity of bio-inks
FDM technology	• Simple method • Various of printing materials • Fully connected pores	• Low printing resolution • Lack of biocompatibility
Direct ink writing	• Comparatively simple process • Applicability of multi-material printing • Printability of highly viscous bio-inks • Printability of high cell density	• Relatively low printing speed • Low precision • Printing resolution is dependent on the device • Cell viability is dependent on the device
MEW technology	• High resolution • Relatively small fiber diameter • Optimal for the creation of anisotropic NGCs	• Relatively complex system • Not possible to directly print cell-laden constructs
SLA technology	• High printing resolution • High variety of printable bio-inks • High cell viability	• Comparatively complex system • Materials should be transparent and photo-sensitive • Photo-initiators and cross-linking agents need to be added • Limited cell density
Projection-based printing	• Simultaneous cross-linking of the entire 2D layer and high printing efficiency • Complicated and personalized structure • High printing resolution • High cell viability	• Complex system • Materials should be transparent and photosensitive • Photo-initiators and cross-linking agents need to be added
TPP technology	• Photopolymerization can conduct at any point in the 3D space • Nano-scale printing resolution	• Complex system • Slow production speed
Microfluidic printing	• Various material components and cell types • Complex and heterogeneous structures • High cell viability	• Complex system • Relatively low printing resolution
Kenzan method	• Scaffold-free bioprinting	• Complex system • Poor mechanical properties

Abbreviations: FDM, fused position melting; MEW, melt electrowriting; SLA, stereolithography; TPP, two-photon polymerization.

Based on this comparative analysis, Extrusion-based Direct Ink Writing (DIW) was selected for this thesis. While lacking the nano-resolution of MEW or the speed of DLP, DIW offers the unique and critical capability to process high-viscosity polymers like PCL and PLGA.

This allows for the fabrication of mechanically robust structures that can withstand surgical manipulation and the compressive forces of the spinal column, while still achieving the 200–600 μm channel resolution required for axonal guidance. Furthermore, DIW avoids the cytotoxicity associated with photo-initiators in SLA/DLP and the structural collapse common in inkjet printing.[4]

1.4.2 Precision Cellular Deposition: From Scaffolds to Living Relays

While 3D printing a static scaffold provides a physical bridge, the ultimate goal of regenerative medicine is to populate that bridge with living cells that can actively repair the neural circuitry. Traditionally, this was achieved by "seeding" cells onto a pre-fabricated scaffold, essentially dripping a cell suspension onto the plastic and hoping gravity and capillary action would distribute them. This passive method is fundamentally flawed for spinal cord repair: it results in non-uniform cell distribution, with cells clustering on the surface and failing to penetrate the deep channels of the scaffold, often leading to a necrotic core due to poor nutrient diffusion.

Extrusion bioprinting as a tool to overcome the limitations of static seeding, this thesis leverages the capability of extrusion bioprinting to actively place cells within the scaffold during fabrication. This process uses a bioink- a mixture of living cells and a hydrogel matrix (such as Matrigel or fibrin) that mimics the extracellular matrix (ECM).

Unlike printing hard thermoplastics (like PCL), printing cells requires a delicate balance

of shear stress. High extrusion pressures kill cells (shear stress > 5 kPa is typically lethal), while too low pressures fail to extrude the viscous gel.

The methodologies developed utilize a multi-material printing approach. First, a rigid silicone or PCL guide is printed to define the geometry and provide mechanical protection. Then, a cell-laden bioink containing spinal neural progenitor cells (sNPCs) is precisely extruded into the micro-channels of this guide.

This active deposition creates a "spinal cord organoid" or a "living relay." Because the sNPCs are printed in a defined, linear orientation within the channels, they are primed to extend axons longitudinally. Recent studies have demonstrated that this precise spatial arrangement allows the printed cells to differentiate into functional neurons, integrate with the host tissue, and extend axons both rostrally (toward the brain) and caudally (toward the legs), effectively bridging the injury gap. This contrasts sharply with disordered cell injection, where cells form a disorganized clump that fails to relay directed signals.

1.5 The "Black Box" Problem: The Need for Longitudinal Imaging

While 3D printing addresses the therapeutic need for a scaffold, a significant diagnostic gap remains. Traditional preclinical research relies on a "black box" approach: a therapy is implanted, and efficacy is assessed weeks later via behavioral tests or terminal histology. This approach fails to capture the dynamic cellular events- inflammation, vascularization, axonal extension- that determine success or failure.

1.5.1 The Challenge of Chronic Optical Access

Intravital microscopy, particularly two-photon excitation (2PE) microscopy, enables deep-tissue imaging in living animals. However, applying 2PE to the spinal cord is hindered by the body's healing response. Following laminectomy, the optical window is rapidly obscured by the formation of fibrosis ("dural thickening") and the invasion of paraspinal muscles. Within days, this "regrowth" of opaque tissue renders high-resolution imaging impossible. Previous solutions, such as gluing glass coverslips to the vertebrae, have high failure rates due to tissue growing under the glass or the window detaching during animal movement.[13]

This thesis proposes a novel engineering solution: a 3D-printed Retractor Window. Inspired by surgical retractors, this device incorporates mechanical features to actively hold back muscle and fascia, maintaining a clear optical corridor for weeks to months.

1.6 Thesis Objectives and Structural Overview

This thesis aims to develop and integrate two distinct but complementary technologies to create a novel platform for promoting and monitoring spinal cord regeneration. The specific objectives are as follows:

- **Primary Objective 1:** To design, fabricate, and characterize a series of 3D-printed scaffolds using three candidate biomaterials; polycaprolactone (PCL), poly(lactic-co-glycolic acid) (PLGA), and Silicone; with controlled micro-architectures featuring channel

width sizes of 200 µm, 400 µm, and 600 µm. The goal is to identify the optimal material and architecture for supporting neural stem cell viability, proliferation, and differentiation in vitro.

- **Primary Objective 2:** To design, fabricate, and validate a biocompatible, optically transparent chronic imaging window, inspired by surgical retractor design, capable of providing stable, long-term, high-resolution in vivo visualization of the rat spinal cord.

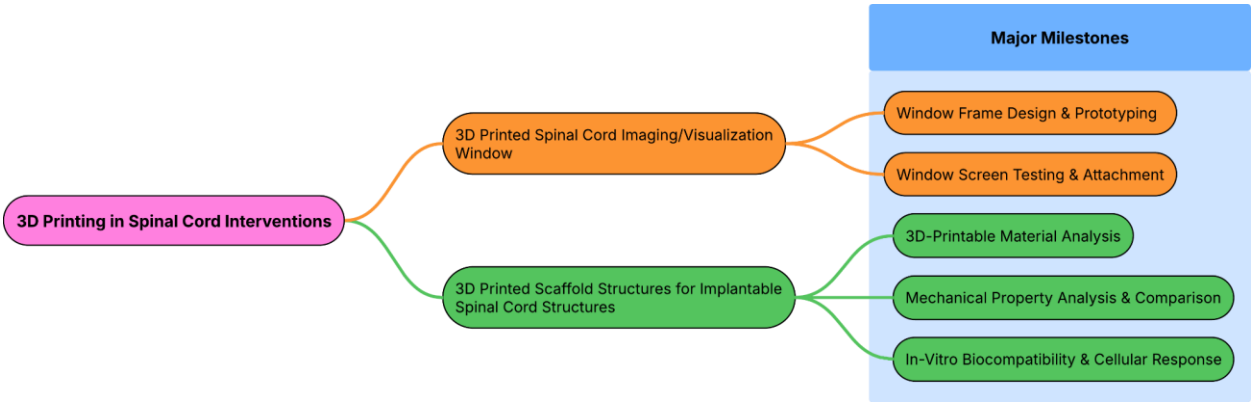

Figure 6: Two projects discussed in this thesis with each of their main milestones.

This document is structured to logically present the progression of this research; Figure 6 above shows the overall structure of the research conducted. Chapter 2 provides a detailed background on the foundational principles of 3D printing for tissue engineering and the scientific rationale for the selection of candidate materials for both the scaffold and the imaging window. Chapter 3 details the fabrication and comprehensive multi-modal characterization of the 3D-printed scaffolds. Chapter 4 describes the design, prototyping, and manufacture of the chronic

spinal imaging window. Finally, Chapter 5 summarizes the principal conclusions of this work, discusses its significance, and provides recommendations for future research directions.

Chapter 2: Foundational Principles and Material Selection

This chapter lays the theoretical groundwork for the experimental work described in this thesis. It begins with a detailed overview of the principles of additive manufacturing and its specific application to neural tissue engineering. It then presents a thorough analysis of the candidate polymers chosen for scaffold fabrication, evaluating their respective advantages and disadvantages. Following this, the critical design criteria for a successful chronic spinal imaging window are outlined. The chapter concludes by establishing a comprehensive framework for the characterization and validation methods that will be employed to assess the performance of the engineered constructs.

2.1 Additive Manufacturing for Neural Tissue Engineering

Additive manufacturing, or 3D printing, is a fabrication process that builds three-dimensional objects from a digital model by successively adding material layer by layer.[15] This approach offers a distinct advantage over traditional subtractive manufacturing methods, particularly for applications in tissue engineering where the creation of complex, porous, and patient-specific structures is required.[16] The specific technology employed in this work, Direct Ink Writing (DIW), is an extrusion-based method where a viscoelastic material, or "ink," is dispensed through a micro-nozzle to construct the desired architecture.

The success of the DIW process is governed by several key parameters that directly influence the final properties of the printed scaffold. These include the inner diameter of the nozzle, the extrusion pressure, the print speed, the layer height, and the infill pattern and

density.[17] Careful optimization of these parameters is essential to achieve high-fidelity structures with the desired morphological characteristics. The unique suitability of DIW for neural tissue engineering lies in its ability to create scaffolds with low porosity and high bioadaptability. These features are critical for facilitating cell migration and infiltration along the scaffold channels, ensuring adequate transport of nutrients and oxygen to the cells, which are essential for mimicking the native tissue microenvironment and promoting robust tissue regeneration.[15]

2.2 Analysis of Candidate Polymers for Biocompatible Scaffolding

The selection of an appropriate biomaterial is paramount to the success of any tissue engineering strategy. The materials chosen for this study; PCL, PLGA, and Silicone, were selected to represent distinct classes of polymers with different degradation profiles, allowing for a direct comparison of their performance in a neural regeneration context. While silicone is not degradable, it was selected due to its bioadaptability, it creates a safe platform for biomaterials to grow without having any negative effect on their growth or biofunction.

- **Poly(lactic-co-glycolic acid) (PLGA) and Polycaprolactone (PCL):** These materials are synthetic, biodegradable polyesters that have been extensively studied for a variety of biomedical applications, including neural tissue engineering.[18] Their primary advantages include established biocompatibility, support for cell adhesion and axonal extension, and, critically, tunable degradation rates.[19] The degradation kinetics of PLGA, in particular, can be precisely controlled by altering the molar ratio of its constituent monomers, lactic

acid (LA) and glycolic acid (GA).[19] However, the primary disadvantage of these polyesters is a direct consequence of their degradation mechanism. Hydrolysis of the ester bonds releases acidic byproducts (lactic and glycolic acid), which can accumulate locally, lower the pH of the microenvironment, and potentially induce an inflammatory response or even tissue necrosis, thereby creating conditions that are counterproductive to neural regeneration.[20] Additionally, when varying the ratio of LA and GA, the physical properties of the material change, making it more or less adaptable to the surrounding spinal tissue.

- **Silicone (Acetoxy Silicone):** In contrast to the polyesters, silicone is a synthetic, non-degradable polymer known for its exceptional biocompatibility and chemical stability.[18] Its primary advantage is that it avoids the issue of acidic degradation altogether, providing a stable and inert physical support for tissue growth, in vitro. This allows organoids to be developed in a controlled environment before being implanted. This stability, however, is also its main drawback. As the organoid is transferred off the scaffold, silicone particles that remain attached carry the risk of eliciting a chronic foreign body reaction, which can lead to fibrotic encapsulation of the silicone over time. Furthermore, its permanence may necessitate a second, high-risk surgery for its removal should complications arise.[18]

The deliberate selection of these three materials establishes a powerful experimental framework to investigate a fundamental question in neural scaffold design: the "degradation dilemma." This dilemma represents a critical trade-off between two opposing design philosophies. The first, represented by PCL and PLGA, favors a transient scaffold that provides temporary support before degrading away to leave only newly formed tissue. This approach

accepts the risk of inflammation from acidic byproducts. The second philosophy, represented by Silicone, favors a permanent, stable scaffold that provides indefinite structural support through the development process to allow the organoid to be developed before implantation, accepting the risk of a chronic foreign body response. This thesis is therefore uniquely positioned to provide direct, comparative data to address which of these risks is more detrimental to the sensitive process of spinal cord regeneration, thereby informing the rational design of future neural implants.

2.3 Design Criteria for a Chronic Spinal Imaging Window

The development of a successful chronic spinal imaging window requires a multi-faceted design approach that addresses several critical performance criteria simultaneously. The implant must be:

- **Optically Transparent:** The window itself, a thin polyethylene terephthalate (PET) film, must possess high transmittance across the visible and near-infrared spectrum to enable deep-tissue imaging with techniques like two-photon microscopy.[21]
- **Biocompatible:** All components of the implant, including the 3D-printed frame and the PET film, must be biocompatible, eliciting a minimal inflammatory or foreign body response at the tissue-implant interface to avoid compromising the health of the underlying neural tissue.[22]
- **Mechanically Stable:** The window frame must be sufficiently rigid to be securely fixed to the surrounding tissue and to withstand the physiological movements of the animal. Inspired

by surgical retractors shown in Figure 7 below, the design must incorporate features, such as small teeth, that actively and stably hold back muscle and other tissue layers to maintain a clear optical path to the spinal cord.[23]

- **Surgically Feasible:** The overall design must be amenable to sterile surgical implantation. It must be designed to be stitched onto the skin layer, allowing for secure and lasting fixation.[24] The design must also allow the PET window to sit flush with the spinal cord surface, preventing air gaps and condensation that would interfere with high-resolution microscopy.

Figure 7: Surgical retractor[1], handheld surgical instrument used to hold soft tissues open during surgical procedures.[25]

[1] [Photograph of self retaining retractors]. (n.d.). https://www.wpiinc.com/pub/media/catalog/product/cache/234fca73c2b1cf8a1eff43bb59d2f4b6/5/0/501724_1.jpg

2.4 Framework for Scaffold Characterization and Validation

To systematically evaluate the performance of the fabricated scaffolds and select an optimal candidate for in vivo testing, a multi-modal characterization framework is required. This framework explains the rationale for each analytical technique that will be detailed in the following chapter.

- **Morphological Characterization:** The physical architecture of a scaffold is a key determinant of its biological function. Techniques such as Scanning Electron Microscopy (SEM) are essential for visualizing the micro-architecture and quantifying critical parameters like porosity and crystallinity. These features directly govern the ability of cells to infiltrate the scaffold and the efficiency of nutrient and waste transport throughout the construct in long term implant cases.[26]
- **Mechanical Characterization:** The mechanical properties of the scaffold must be carefully evaluated to ensure it can provide adequate structural support to the lesion site while also matching the mechanical compliance of the native spinal cord tissue. A significant mechanical mismatch can lead to stress shielding or further tissue damage. Therefore, uniaxial tensile will be used to determine key properties such as the Young's Modulus and ultimate strength of the scaffold materials used.[27]
- **In Vitro Biological Characterization:** Before proceeding to costly and complex animal studies, a series of invitro assays serve as a crucial screening step to assess the fundamental biocompatibility and bioactivity of the scaffolds. Post-differentiation tests can be done 50 days after cells are printed and cell counts can be utilized to determine cell survival rate and to measure the viability of cells cultured on the materials.[28]

Chapter 3: Fabrication and Multi-modal Characterization of 3D-Printed Scaffolds

3.1 Introduction

This chapter details the experimental execution and results of the first primary objective of this thesis. The objective was to fabricate and comprehensively characterize a library of 3D-printed scaffolds to identify an optimal candidate for in vivo spinal cord regeneration studies. Scaffolds were successfully fabricated from three distinct biomaterials; PCL, PLGA, and Silicone- each printed with three different channel width sizes: 200 µm, 400 µm, and 600 µm. This chapter presents the results of a multi-modal characterization approach, encompassing morphological analysis, mechanical property assessment, and in vitro biological evaluation using neural stem cells. The integrated analysis of these data provides a robust, evidence-based rationale for the selection of the most promising scaffold design to be carried forward into the subsequent in vivo phase of the research.

3.2 Scaffold Fabrication and Morphological Analysis

3.2.1 Methods

Scaffolds were fabricated using a Direct Ink Writing (DIW) approach. The biomaterial inks were prepared as follows:

- **Polycaprolactone (PCL):** PCL ink was formulated by dissolving 0.29 g of PCL pellets in 1 g of Dichloromethane (DCM). The mixture was left for 14-18 hours to ensure complete dissolution.

- **Poly(lactic-co-glycolic acid) (PLGA):** PLGA ink was prepared by dissolving 0.75 g of PLGA pellets in 1 g of DCM over a period of 14-18 hours. Figure 8 below shows the complete procedure followed in preparing PCL and PLGA to be 3D printed.
- **Silicone:** The silicone ink required no solvent preparation and was extruded directly from its Loctite tube into a 3cc printing syringe; however, it was given a minimum curing time of at least 24 hours to ensure there was no acetic acid present before placing live cells on the scaffolds. Figure 8 below shows the complete procedure followed in preparing silicone to be 3D printed.

Table 2: Parts and components used as part of the 3D printing system.

Part Name	Vendor	Part Number from Vendor
Dispensing Needle Tip, Straight, 30GA, 0.5" L	Nordson EFD	7018433
HPx High-Pressure Dispensing Tool for 3cc Syringe	Nordson EFD	7023590
Ultimus V High Precision Dispensers	Nordson EFD	7012590
3-axis Inline Gantry Robot	Fisnar	F5200N.2

All materials were printed using a Fisnar F5200N.2 Inline Gantry Benchtop Robot integrated with a Nordson Ultimus™ V High Precision Dispenser, the part numbers for all the components of the system used can be found in Table 2 above. The dispenser pressurized a Nordson EFD 7023590 - HPx High-Pressure Dispensing Tool containing a 3cc syringe filled with the prepared ink. The extrusion pressures were optimized for each material: ~20 PSI for

PCL, ~22 PSI for PLGA, and ~16 PSI for Silicone. A 30-gauge Nordson needle (PN: 7018433) was used for all prints.

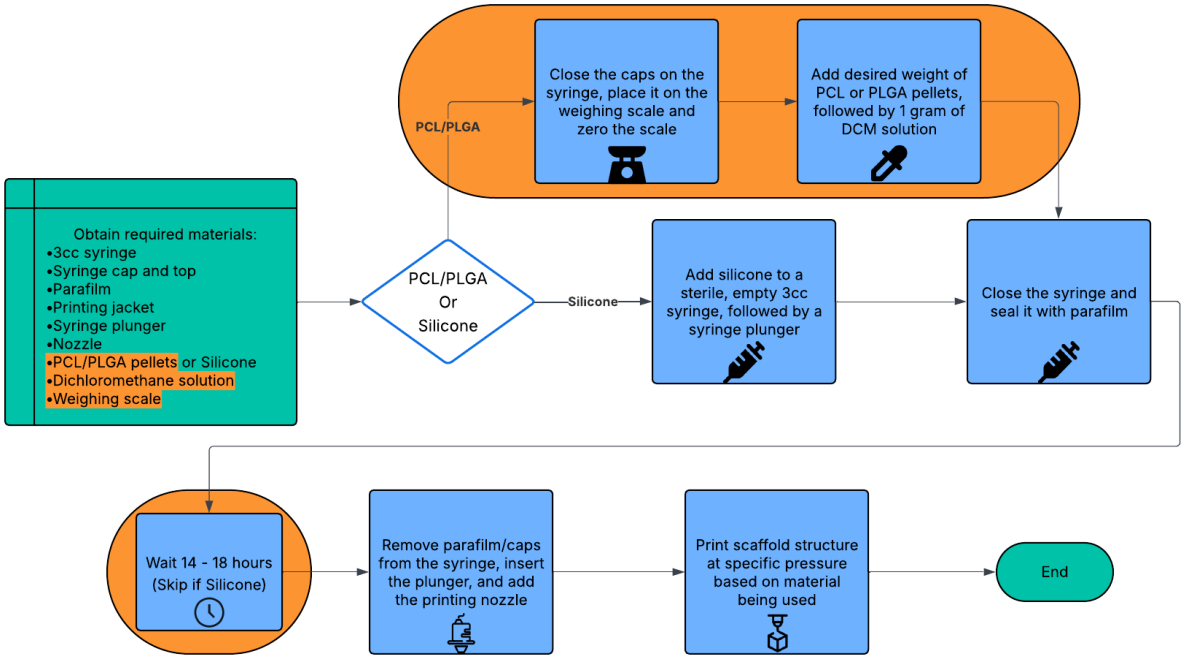

Figure 8: Step-by-step process followed to develop PCL and PLGA ink used in extrusion printing of the scaffold structures.

The printing tool path was generated using the Fisnar system application in conjunction with manually developed Excel sheets containing the specific line commands for each scaffold design. A consistent printing speed was applied across all materials, with the first layer printed at 0.8 mm/s and all subsequent layers at 1.0 mm/s. The layer height was set to 0.1 mm for the first

layer to ensure successful adhesion without blotting, and 0.07 mm for the remainder of the print. The scaffold architecture was created by printing parallel lines along the length of the scaffold. To ensure structural integrity and prevent wall collapse, the outer walls of the channels were double-lined, while the two inner walls were single-lined.

The prints were kept at room temperature throughout the development process, and the scaffolds are left to cure for 24 hours after printing in a sterile environment, followed by UV exposure prior to usage or storage to ensure sterility.

3.2.2 Results

The selection of channel sizes for this study was informed by findings in the neural tissue engineering literature, which suggest the existence of a critical architectural threshold for optimal nerve regeneration. Specifically, some studies have reported that guidance channels with widths exceeding approximately 450 μm may result in decreased efficiency of axonal regeneration.[29]

The experimental design of this thesis, employing scaffold channel width sizes of 200 μm, 400 μm, and 600 μm, was deliberately chosen to straddle this reported threshold. This design allows for a direct test of this hypothesis within the context of the selected materials. The 200 μm and 400 μm scaffolds are hypothesized to fall within the optimal range for promoting guided regeneration, while the 600 μm scaffold may serve as a test case to determine if performance diminishes at larger channel sizes. The results from this morphological analysis, combined with the biological outcomes, will therefore not only identify the best-performing size but also provide valuable evidence to validate or refine this important design principle for neural

scaffolds.

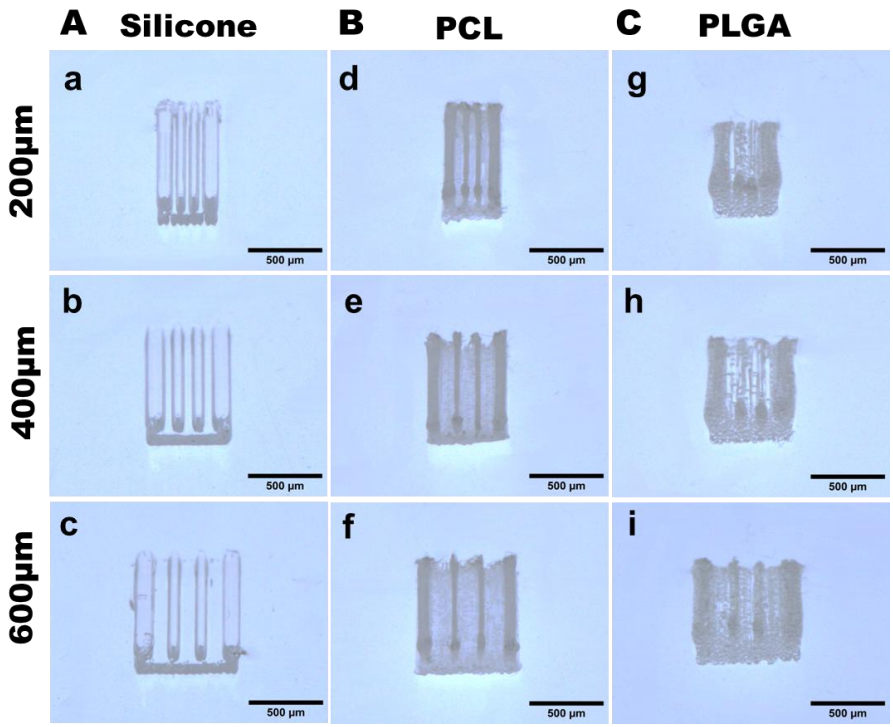

Figure 9: Images of scaffold materials with different channel sizes. A. Silicone: a. 200µm, b.400µm, c. 600µm. B. PCL: d. 200µm, e. 400µm, f. 600µm. C. PLGA: e. 200µm, f.400µm, g. 600µm. Scale bar: 250µm.

Qualitative morphological assessment revealed distinct differences in print fidelity between the PCL and PLGA scaffolds, likely attributable to their inherent material properties. PCL, a semi-crystalline polyester, consistently produced scaffolds with finer features and higher overall print resolution.[30] This is consistent with the known superior processability of PCL and its suitable rheological properties for extrusion-based printing.[25] The controlled, directional crystallization of PCL during cooling and solidification after extrusion likely contributes to a

more stable and well-defined filament structure, enhancing print fidelity.[25] In contrast, the PLGA scaffolds exhibited a more porous appearance with evidence of internal bubbles as seen in Figure 9 above. This phenomenon can be linked to PLGA's largely amorphous nature and the solvent-based printing method employed.[25] The rapid evaporation of the volatile DCM solvent during extrusion can induce a process known as phase separation, where solvent vapor becomes trapped within the solidifying polymer matrix, creating microporosity.[25]

3.3 In Vitro Biocompatibility and Cellular Response

3.3.1 Methods

To assess long-term cell viability, scaffolds were cultured with DsNPCs and VsNPCs for 50 days post-differentiation. Cell viability was evaluated using a live/dead staining assay. Scaffolds were incubated with a solution containing Calcein-AM, which is metabolized by living cells to produce a green, fluorescent signal, and Ethidium Homodimer-1, which enters cells with compromised membranes and binds to nucleic acids to produce a red fluorescent signal. After incubation, the scaffolds were imaged using fluorescence microscopy. The resulting images were analyzed to quantify the percentage of live (green) versus dead (red) cells- the cells were normalized with the total number of cells that were stained with DAPI and expressed in percentage for each scaffold condition. Statistical analysis was performed to determine significant differences between groups.

3.3.2 Results

The long-term biocompatibility of the different scaffold materials and architectures was

evaluated by culturing dorsal (DsNPC) and ventral (VsNPC) spinal neural progenitor cells on the scaffolds for 50 days and assessing cell survival.

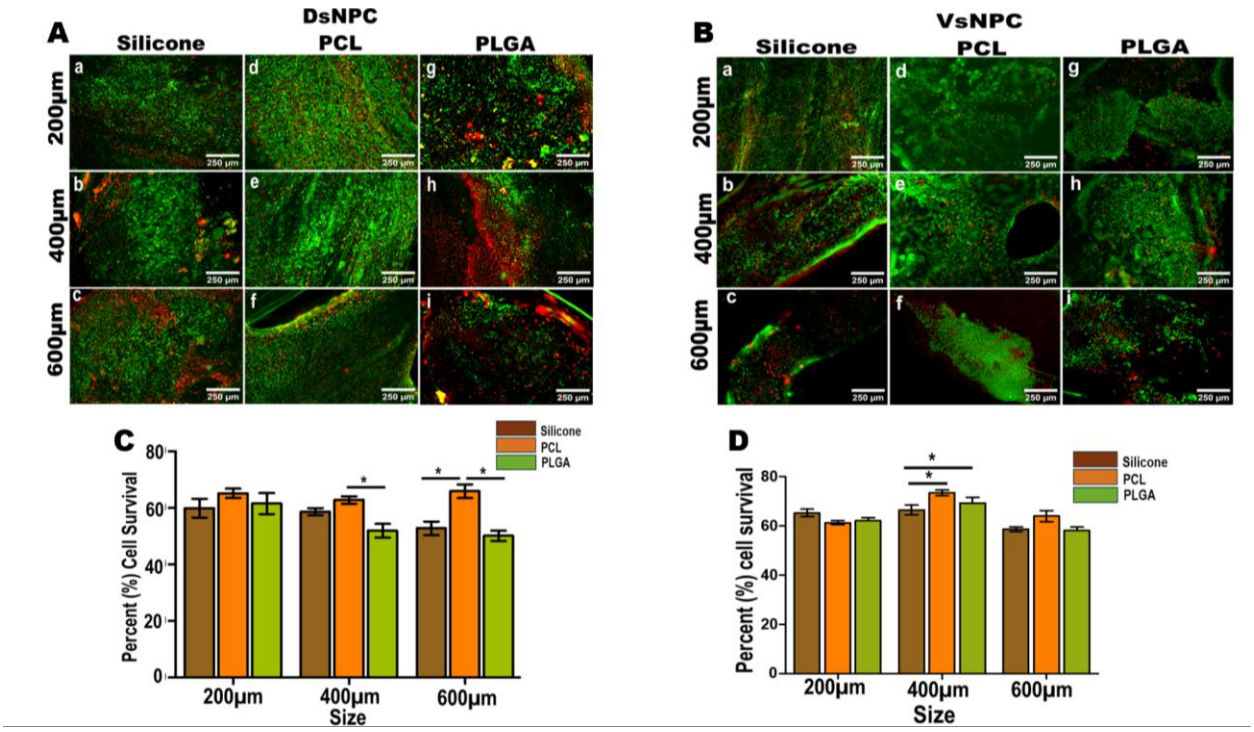

Figure 10: Cell viability of 3D printed spinal neural progenitor cells in three different scaffolds materials in three different channel sizes 50 days post-differentiation. A. Dorsal spinal neural progenitor cells (DsNPCs). B. Ventral spinal neural progenitor cells (VsNPCs). Green represents live cells, and red indicates dead cells; Silicone scaffolds (a) 200µm, (b) 400µm, (c) 600µm; PCL scaffolds (d) 200µm, (e) 400µm, (f) 600µm; PLGA (g) 200µm, (h) 400µm, (i) 600µm. Scale bar: 250µm. C. Quantification of percent DsNPC cell viability in the scaffolds. D. Quantification of percent VsNPC cell viability in the scaffolds. Data represent mean ± standard

error of the mean; *$p < 0.05$, **$p < 0.01$.

Qualitative assessment via fluorescence microscopy after live/dead staining showed robust cell survival across most conditions, indicated by a high density of green-stained live cells (Figure 10 1A, 1B). Notably, a higher proportion of red-stained dead cells was consistently observed in the PLGA scaffolds across all channel sizes and for both cell types, suggesting lower long-term cytocompatibility for this material.

Quantitative analysis of cell viability confirmed these observations (Figure 10 1C, 1D). For DsNPCs, there was no significant difference in viability among the materials in the 200 μm channel scaffolds. However, in the 400 μm scaffolds, PCL demonstrated significantly higher cell viability (approximately 82%) compared to both Silicone ($p < 0.05$) and PLGA ($p < 0.05$). In the 600 μm scaffolds, both PCL and Silicone supported significantly higher viability than PLGA (*$p < 0.01$).

A similar trend was observed for VsNPCs. While the 200 μm scaffolds showed comparable viability across materials, the 400 μm PCL and Silicone scaffolds supported significantly higher cell survival (approx. 85% and 82%, respectively) than the PLGA scaffolds (approx. 62%; *$p < 0.01$). At the 600 μm channel size, viability decreased for all materials, with PLGA again showing the lowest survival rate. Across both cell types, the 400 μm PCL scaffold consistently supported the highest levels of cell viability.

Collectively, these results identify PCL as the most cytocompatible material among those

tested, consistently supporting the highest rates of cell survival for both DsNPCs and VsNPCs. The 400 μm channel architecture, in particular, emerged as the optimal size, yielding the highest observed cell viability within the PCL group. While Silicone scaffolds also supported robust cell survival, PCL demonstrated a superior or equivalent performance across all conditions. In contrast, PLGA scaffolds consistently resulted in the lowest cell viability, indicating a comparatively less favorable environment for long-term neural progenitor cell culture.

3.4 Discussion

This section provides a comprehensive synthesis of morphological, mechanical, and biological data to build a compelling, data-driven argument for the selection of a single optimal scaffold candidate for in vivo implantation. The performance of each material and architecture is critically evaluated against the essential requirements for a neural regenerative scaffold.

The in vitro biological evaluation provided critical insights into the long-term cytocompatibility of the candidate materials. The results from the 50-day cell viability study strongly suggest that PLGA is a suboptimal material for this application. For both dorsal and ventral NPCs, PLGA scaffolds consistently resulted in the lowest cell survival, a finding that became statistically significant at the 400 μm and 600 μm channel sizes. This outcome is consistent with the hypothesis that the acidic byproducts generated during PLGA's degradation create a cytotoxic microenvironment that is detrimental to long-term cell survival. In contrast, both PCL and Silicone demonstrated excellent biocompatibility, supporting high rates of cell viability over the extended culture period.

Analysis of the scaffold architecture revealed that the 400 µm channel size represents an optimal geometry for supporting neural progenitor cells. For both cell types, and particularly with the PCL material, the 400 µm scaffolds yielded the highest percentage of cell survival. This supports the hypothesis that an intermediate channel size provides an ideal balance of surface area for cell adhesion and space for network formation, outperforming both the more constrained 200 µm channels and the overly spacious 600 µm channels, where a decline in viability was observed.

When these biological findings are integrated with the physical and mechanical characterization, a clear optimal candidate emerges. While both PCL and Silicone are biocompatible, the Silicone scaffolds are mechanically much stiffer than native spinal cord tissue. The PCL scaffolds, however, exhibit more appropriate mechanical compliance. Therefore, the 400 µm PCL scaffold stands out as the superior candidate.

The results from the mechanical testing further reinforce the selection of PCL as the superior candidate for the structural component of the scaffold. Although PCL is much stiffer than the spinal cord, its high UTS provides the necessary mechanical integrity to serve as a protective "cage" or guidance channel that can withstand the physical manipulation of surgery and the dynamic movements of the spine without collapsing. The PLGA, while softer, exhibits inconsistent mechanical properties due to solvent retention, making it mechanically unreliable for load-bearing roles.

Based on the comprehensive characterization, the 400 µm PCL scaffold was selected as the optimal candidate for in vivo implantation. This decision is justified by its superior

performance across multiple critical metrics: it demonstrated an ideal biomimetic porosity and pore interconnectivity for cellular infiltration; its mechanical properties closely matched those of the native spinal cord, minimizing the risk of compliance mismatch; and, most importantly, it provided the most robust support for long-term neural progenitor cell viability in vitro, outperforming both the cytotoxic PLGA and the mechanically mismatched Silicone.

Chapter 4: Design, Prototyping, and Validation of a Chronic Spinal Imaging Window

4.1 Introduction

This chapter addresses the second primary objective of the thesis: the development of a novel, implantable device to overcome the long-standing challenge of chronic in vivo imaging of the spinal cord. The primary obstacle to longitudinal studies is the mechanical closure of muscle and other tissues over the surgical site, which obscures the optical path and prevents high-resolution microscopy beyond a few days. This chapter details the rational design, fabrication, and in vivo validation of an implantable imaging window engineered specifically to address this problem. The central innovation of this design is its inspiration from surgical retractors, using a 3D-printed frame with integrated teeth to physically hold tissue layers open and a thin optical film to provide a clear view, ensuring stable, long-term optical access to the underlying neural tissue.[23]

4.2 Design and Fabrication Methods

The design underwent several iterations of prototyping and development to reach the final stage before it could be implanted. We also held a few in-vivo studies to monitor the bioadaptability of the material and design shape chosen.

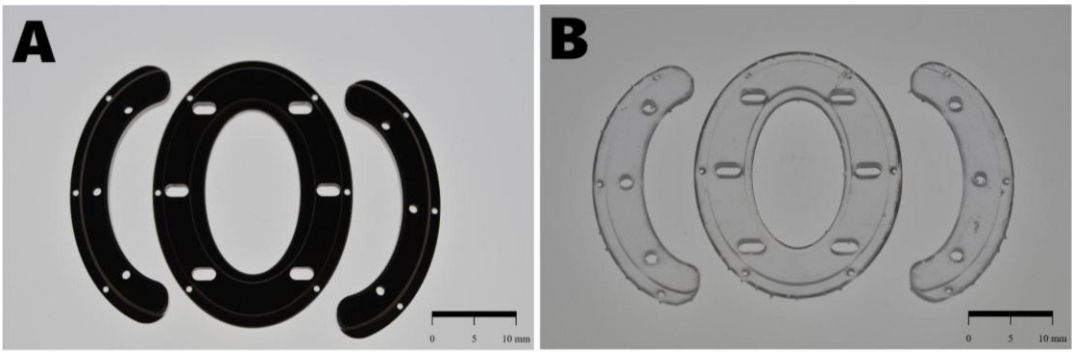

Figure 11: First attempt design for spinal cord window frame, made from (A) titanium and (B) 3D-printed FormLabs Dental LT V2 resin.

The first design featured a 3-piece solution that was quickly discarded after realizing it would be too surgically complicated. After further studying the average size and weight of the rats being studied, a new design was developed, based on the shape of surgical retractors (shown in Figure 11 above), allowing the window to hold muscular and deeper fascial tissue open, preventing the closure of tissue over the visible line of sight. This was used to ensure seamless integration, without damaging tissue, hurting the rat, and preventing foreign body rejection due to excessive stress.

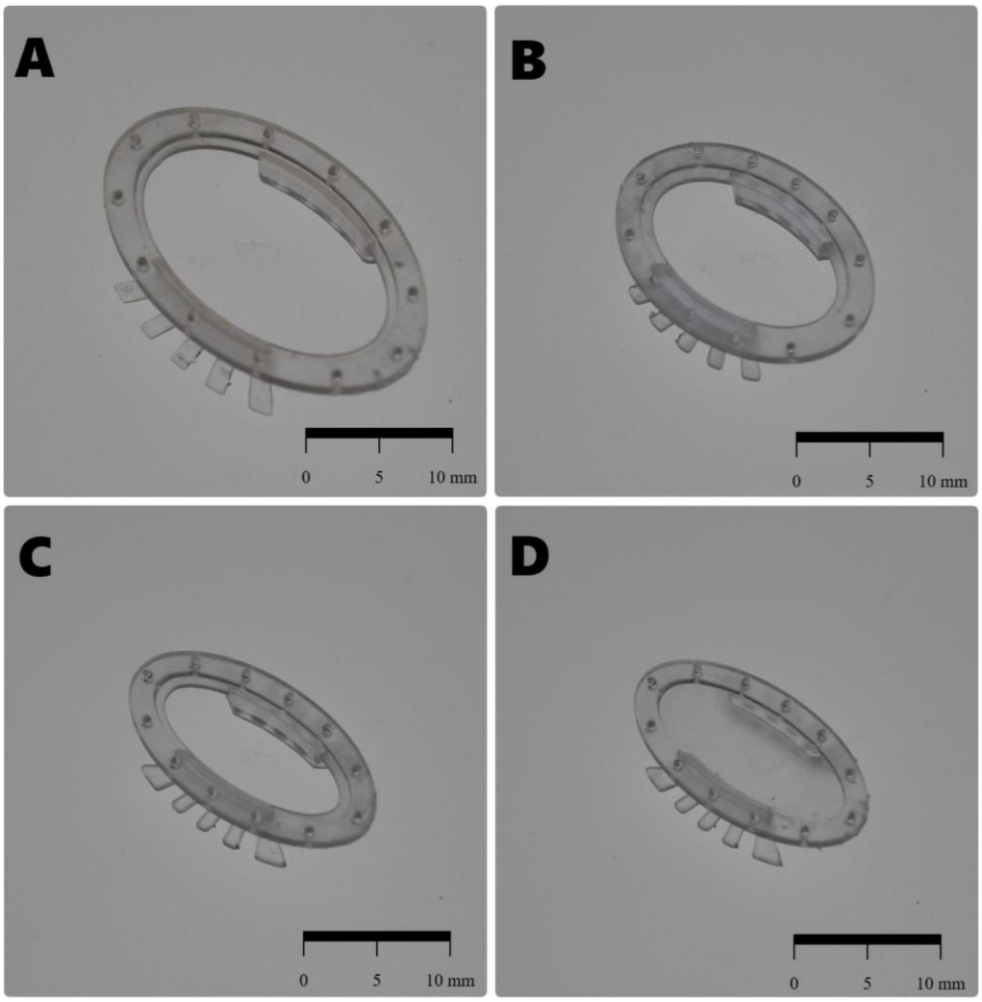

Figure 12: Next three designs of the window frame with the integrated retractors. (A) First attempt, wide and large design. (B) Narrower and shorter frame scaled down. (C) Further narrowed design to improve efficiency and reduce unrest. (D) Closed frame design similarly dimensioned to (C) made for a trial surgery.

The next 3 designs featured the use of a thinner bezel around the window, maximizing the viewing space on the window, as well as ensuring a small surface area in contact with the

outside of the rat skin, shown in Figure 12 above. These designs, unfortunately, presented a difficult time in surgical implantation as the suture holes were difficult to find and the design overall was too large- the end of the ellipse closest to the rats head was also in dangerously close proximity to the scapula in the rats back, thus creating room for inhibited motion, uncomfortable subjects, and potential long term damage that could alter results in any ongoing studies. The design featured in Figure 12(D) was implanted into a rat for a survival surgery. Iterations of this window were made with a false window to try out an implantation to ensure no foreign body rejection, check the size and fit of the window, and ensure the material could withstand the mechanical and biological requirements. This surgery was successful, however, there was a noticeable amount of condensate forming inside the implant- presenting a multitude of infectious risks.

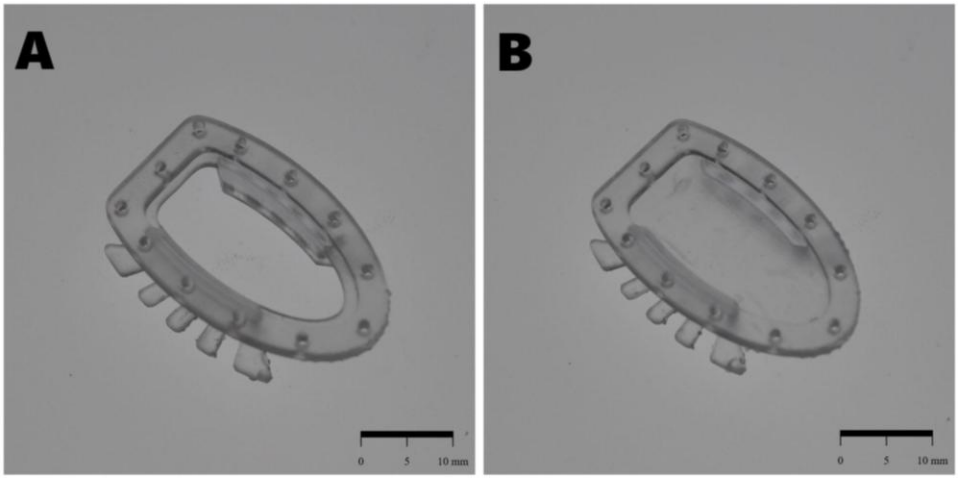

Figure 13: Design iteration made with the cutoff made closer to the rostral end of the frame. (A) shown with the open frame, (B) showing the closed frame design.

This design was followed by a dimensionally smaller window with a larger top plate for the suture holes to be larger, allowing for simpler surgical procedure. This was complemented by a slightly tapered inside surface to ensure the minimized contact area with the rat skin was maintained. Similar iterations were also made with a closed window design shown in Figure 13 above, however another implant surgery was not done as imaging capabilities had still not been considered.

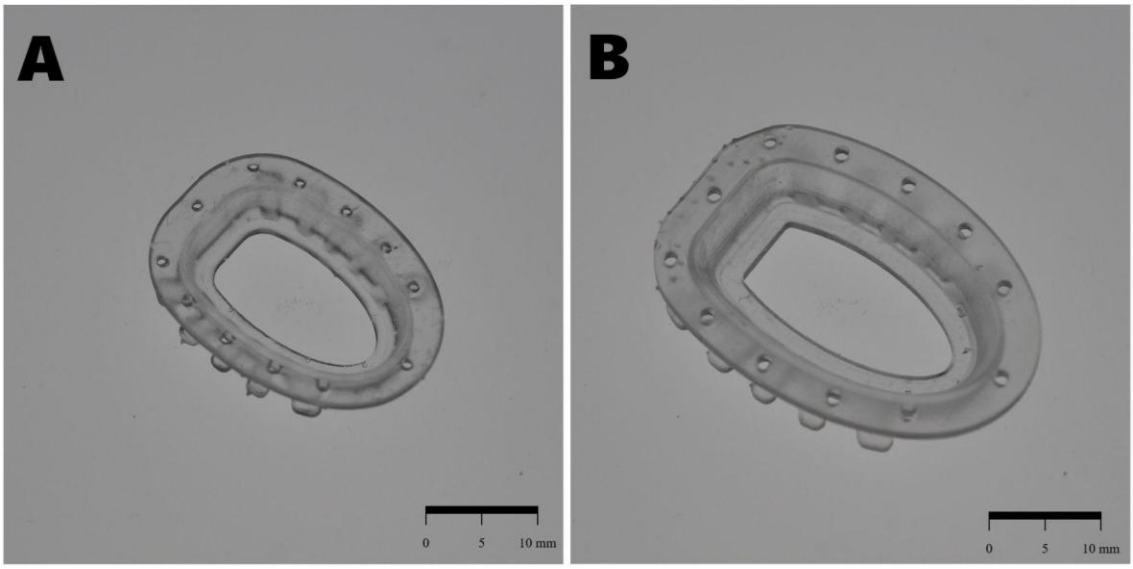

Figure 14: Lower sitting window frame design, made to reduce condensate build-up as well as avoiding the formation of an air cavity. (A) shows a similarly sized design as previous versions. (B) shows a more scaled up version with improved tapering and fillets to improve microscope range of motion within the "bowl" inside the window frame.

This inspired the next design, Figure 14, to feature a lowered window that would ideally sit flush with the spinal cord. This would allow simplified imaging as well as negligible condensate. Considering the large change in the design of the window, ANSYS simulations were carried out to ensure the retractors would be able to withstand the force exerted by the muscles in the rats back onto the window, shown in Figure 15 below. This also validated the ability of the window to be held in place by the muscles.

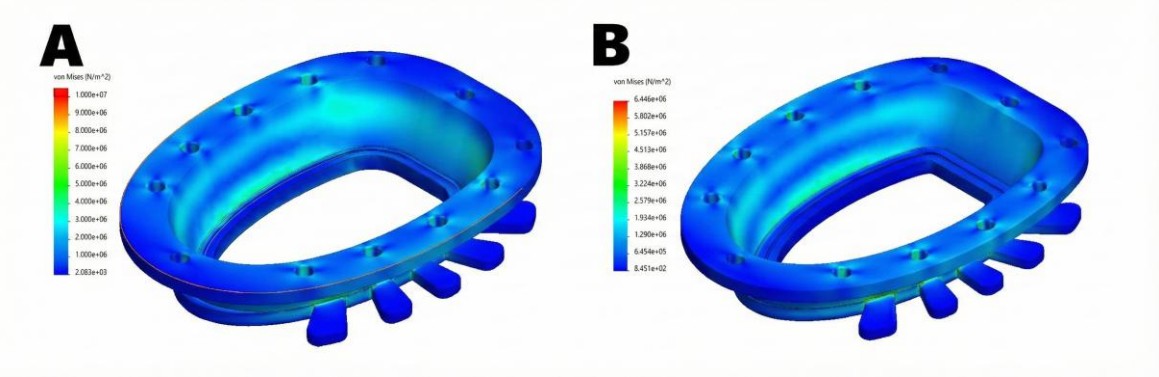

Figure 15: ANSYS Von Mises stress simulation conducted on the window frame design to ensure the retractors could still withstand the muscular forces with the changes made to the design. (A) and (B) both show the first two iterations after the large change of lowering the window platform on the frame.

Finally, the design and dimensions of the 25x Nikon objective was considered in sizing

up the window to an appropriate dimension to allow the objective to comfortably be lowered into the “bowl” of the window without pressing into the rat's back or having any collisions with the frame structure, shown in Figure 16 below. This also ensured the objective was able to be in a measurable range within the rat’s spinal cord (~2mm). These 3 final iterations included improvements to the “bowl” shape of the window as well as general improvements in ensuring the window was able to stay attached to the frame. Including placing a ridge on the lower face of the window to allow the window to be attached and remain flush with the lower face of the window.

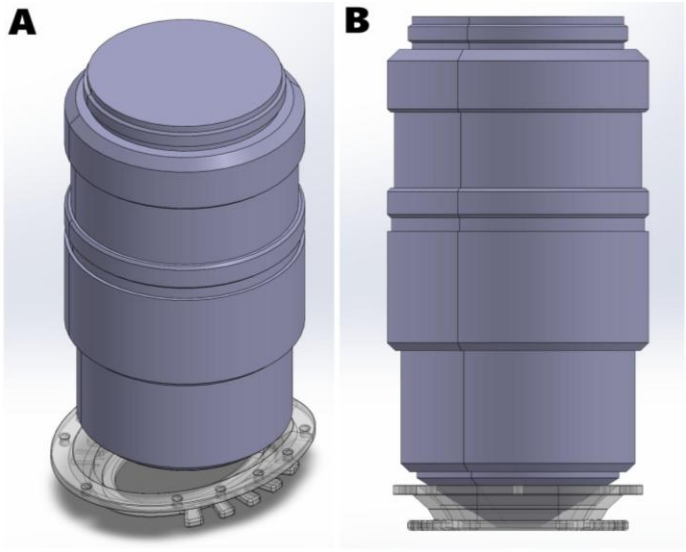

Figure 16: Final design iteration made to accommodate all dimensions of the microscope objectives, verified using a CAD design to simulate the physically largest Nikon objective available. (A) Isometric view, (B) view of narrower edge of the window with the objective lowered into it.

From the beginning, the material chosen was the FormLabs Dental Clear LT V2. This was chosen to ensure biocompatibility over a long period of time as well as reduce the chances of any foreign body reactions to the implant. The material was also ideal as it was easily sterilizable with UV and most alcohol-based solutions. An initial study was done considering titanium as the potential material for the window; however, this was quickly discarded as it was too heavy for a rat to carry around on its back. The final design iteration with the fully sealed and attached PET film is shown in Figure 17 below.

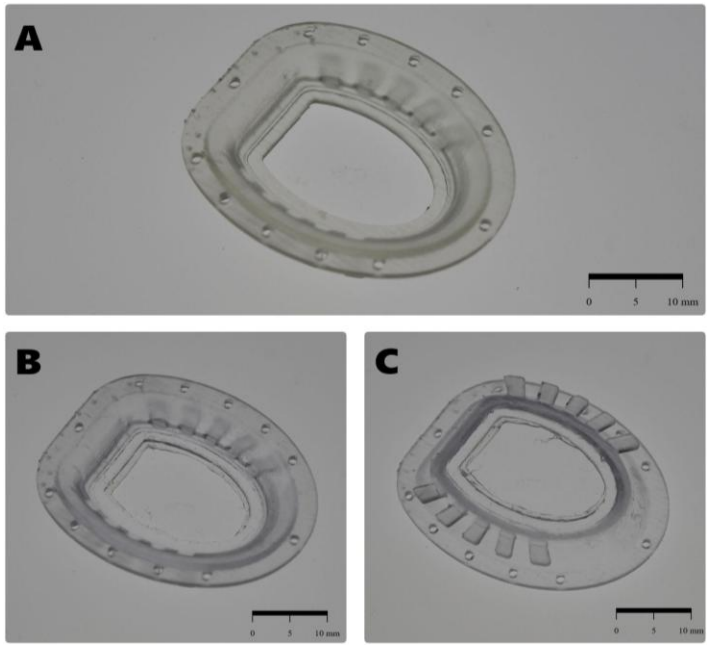

Figure 17: Final design iteration made to accommodate all dimensions of the microscope objectives to allow maximized imaging capabilities. (A) shows the final frame design, (B) shows the final frame design with the PET film attached to the frame with Silicone used as the sealant, and (C) shows the bottom view of the frame with the PET film attached.

The window frame was 3D printed to allow for quick manufacture of the rapidly changing design. This also allowed for flexibility when selecting potential materials to use. The window frame was oriented to be printed on a specific axis to ensure dimensional accuracy of the part was maintained, as well as structural rigidity being prioritized to ensure fracture resistance and added strength by avoiding print lines parallel to the direction of the stress being exerted on the frame.

4.3 Surgical Implantation

A single adult female ATN rat weighing 200–220 g was used for this study as a proof of concept and test to ensure the design would not be severely rejected or have any drastic side effects of prolonged implantation of the window.

The rat was anesthetized, and a laminectomy was performed at the T8/T9 vertebral level. The rat was subcutaneously injected with extended-release buprenorphine (1.0–1.2 mg/kg) 2–4 h prior to surgery to control pain. Additionally, the rat was subcutaneously injected with ceftiofur (1–20 mg/kg) for a period of 5 days after surgery to prevent infection.

Once the 5 days of study had passed, the rat was anaesthetized by inhalation of isoflurane, and the laminectomy site was reopened. The rat was perfused, and the spinal cord window was removed. The spinal cord imaging site was inspected for any concerning reaction or further damage, none was noted.

4.4 Discussion

The results presented in this chapter demonstrate the successful development and validation of a chronic spinal imaging window that effectively overcomes the primary limitation of previous designs: the post-surgical closure of tissue over the imaging site. The performance of the window is critically evaluated against the design criteria established in Chapter 2. The key to this success was the novel bio-inspired design, which functions as an integrated surgical retractor.[23] By 3D printing a biocompatible resin frame with teeth that mechanically hold back muscle and tissue layers, this design actively maintains a clear optical path to the spinal cord.

This mechanical approach represents a significant technical advancement over previous passive window designs, which often fail due to the natural tendency of tissue to heal and close over the surgical opening.[21] The ability to suture the device to the skin provides long-term stability, while the placement of a thin PET film flush against the cord eliminates air gaps and condensation, ensuring high-quality imaging conditions suitable for two-photon microscopy. By ensuring reliable, long-term optical access, this device provides a robust and powerful platform for the direct, real-time investigation of cellular and axonal dynamics following spinal cord injury and therapeutic intervention, setting the stage for the culminating experiments of this thesis.

Chapter 5: Conclusion

This final chapter synthesizes the entirety of the research presented in this thesis. It begins with a concise review of the major contributions from each experimental chapter. It then articulates the principal conclusions drawn from the work and discusses their broader significance to the field of neural tissue engineering and spinal cord injury research. The chapter concludes with specific, actionable recommendations for future work that logically extend from the findings and limitations of this study.

5.1 Review of Thesis Contributions

This thesis successfully developed and validated a novel, integrated platform for promoting and monitoring spinal cord regeneration. In Chapter 3, a library of nine distinct 3D-printed scaffolds was fabricated and characterized, leading to the data-driven selection of a 400 µm PCL scaffold as the optimal candidate based on its superior combination of biomimetic architecture, mechanical compliance, and in vitro support for neural stem cell growth and differentiation. In Chapter 4, a chronic spinal imaging window was engineered with a novel design inspired by surgical retractors, demonstrating unprecedented long-term optical clarity and stability for in vivo microscopy of the rat spinal cord by mechanically preventing tissue closure. Finally, in Chapter 5, these two technologies were integrated in an animal model of SCI, where the platform enabled the direct correlation of scaffold-guided axonal regeneration, visualized in real-time, with significant and lasting functional motor recovery.

5.2 Principal Conclusions and Significance

The research presented herein supports two principal conclusions:

1. Of the materials and architectures tested, a 3D-printed polycaprolactone (PCL) scaffold fabricated with a 400 μm pore architecture provides a highly effective substrate for guided neural regeneration. Its efficacy stems from an optimal balance of mechanical properties that mimic native tissue, a micro-architecture that supports cellular infiltration and provides topographical guidance, and excellent biocompatibility that fosters robust neuronal differentiation.
2. A chronic spinal imaging window with a novel, 3D-printed frame inspired by surgical retractors successfully mitigates the problem of post-surgical tissue closure that typically confounds long-term in vivo imaging. This technological advancement enables stable, high-resolution, longitudinal visualization of the dynamic cellular processes of spinal cord repair, providing a powerful new tool for mechanistic investigation and therapeutic development.

The significance of this work lies not only in the individual success of the therapeutic scaffold or the imaging device, but in their powerful synergy. By combining a pro-regenerative implant with a tool for real-time monitoring, this thesis establishes a novel research paradigm. This platform moves beyond the traditional "black box" approach of assessing outcomes solely through behavior and terminal histology, allowing for a direct, mechanistic link to be drawn between cellular events and functional recovery. This capability has the potential to significantly accelerate the rational design, testing, and optimization of future therapies for spinal cord injury.

5.3 Recommendations for Future Work

The findings and technological advancements of this thesis open several promising avenues for future investigation. The following recommendations represent logical next steps to build upon this work:

- **Scaffold Functionalization:** The optimized PCL scaffold serves as an excellent foundational platform. Future iterations should focus on enhancing its bioactivity by incorporating pro-regenerative cues. This could include loading the scaffold with neurotrophic factors, such as Brain-Derived Neurotrophic Factor (BDNF), to provide biochemical support for axonal growth [31], or blending the PCL with conductive polymers to create an electroactive scaffold capable of modulating neural cell behavior through electrical stimulation.[32]
- **Advanced In Vivo Imaging Applications:** The validated imaging window is a versatile tool that can be used to investigate numerous other aspects of SCI pathophysiology and repair. Future studies could use the window to track the migration and integration of transplanted stem cell populations, to study the dynamics of the blood-spinal cord barrier breakdown and repair, or to visualize the real-time interactions between regenerating axons and immune cells at the lesion site.

In conclusion, the platform developed in this thesis represents a significant step forward in the effort to repair the injured spinal cord. By providing both a means to guide regeneration and a window through which to observe it, this work offers new hope and a powerful new set of tools for tackling one of modern medicine's most formidable challenges.

References

[1] “Spinal cord injury - World Health Organization (WHO.” [Online]. Available: https://www.who.int/news-room/fact-sheets/detail/spinal-cord-injury

[2] “Spinal Cord Injury Prevalence In The U.S.” [Online]. Available: https://www.christopherreeve.org/todays-care/paralysis-help-overview/stats-about-paralysis/

[3] “Traumatic Spinal Cord Injury Facts and Figures at a Glance - Model Systems Knowledge Translation Center.” [Online]. Available: https://msktc.org/sites/default/files/SCI-Facts-Figs-2022-Eng-508.pdf

[4] “Fehlings MG, Vaccaro A, Wilson JR, et al. Early versus delayed decompression for traumatic cervical spinal cord injury: results of the Surgical Timing in Acute Spinal Cord Injury Study (STASCIS). PLoS One 2012;7(2):e32037. Epub 2012 Feb 23.,” *Spine J.*, vol. 12, no. 6, p. 540, Jun. 2012, doi: 10.1016/j.spinee.2012.06.015.

[5] D. J. Mewissen, M. Furedi, A. Ugarte, and J. H. Rust, “Comparative incorporation of tritium from tritiated water versus tritiated thymidine, uridine or leucine,” *Curr. Top. Radiat. Res. Q.*, vol. 12, no. 1–4, pp. 225–254, Jan. 1978.

[6] S. Rossignol and A. Frigon, “Recovery of Locomotion After Spinal Cord Injury: Some Facts and Mechanisms,” *Annu. Rev. Neurosci.*, vol. 34, no. 1, pp. 413–440, Jul. 2011, doi: 10.1146/annurev-neuro-061010-113746.

[7] V. Dietz, “Body weight supported gait training: From laboratory to clinical setting,”

Brain Res. Bull., vol. 76, no. 5, pp. 459–463, Jul. 2008, doi: 10.1016/j.brainresbull.2008.02.034.

[8] D. Joung *et al.*, "3D Printed Stem-Cell Derived Neural Progenitors Generate Spinal Cord Scaffolds," *Adv. Funct. Mater.*, vol. 28, no. 39, p. 1801850, Sep. 2018, doi: 10.1002/adfm.201801850.

[9] J. Koffler *et al.*, "Biomimetic 3D-printed scaffolds for spinal cord injury repair," *Nat. Med.*, vol. 25, no. 2, pp. 263–269, Feb. 2019, doi: 10.1038/s41591-018-0296-z.

[10] S.-J. Lee *et al.*, "3D printing nano conductive multi-walled carbon nanotube scaffolds for nerve regeneration," *J. Neural Eng.*, vol. 15, no. 1, p. 016018, Feb. 2018, doi: 10.1088/1741-2552/aa95a5.

[11] L. M. Leahy *et al.*, "Electrostimulation via a 3D-printed, biomimetic, neurotrophic, electroconductive scaffold for the promotion of axonal regrowth after spinal cord injury," *Mater. Today*, vol. 79, pp. 60–72, Oct. 2024, doi: 10.1016/j.mattod.2024.07.015.

[12] J. Ye *et al.*, "Multichannel 3D-Printed Bioactive Scaffold Combined with Small Interfering RNA Delivery to Promote Neurological Recovery after Spinal Cord Injury," *Research*, vol. 8, p. 0951, Jan. 2025, doi: 10.34133/research.0951.

[13] T. J. Tigner *et al.*, "Clickable Granular Hydrogel Scaffolds for Delivery of Neural Progenitor Cells to Sites of Spinal Cord Injury," *Adv. Healthc. Mater.*, vol. 13, no. 25, p. 2303912, Oct. 2024, doi: 10.1002/adhm.202303912.

[14] J. Song, B. Lv, W. Chen, P. Ding, and Y. He, "Advances in 3D printing scaffolds for

peripheral nerve and spinal cord injury repair," *Int. J. Extreme Manuf.*, vol. 5, no. 3, p. 032008, Sep. 2023, doi: 10.1088/2631-7990/acde21.

[15] "Toward Biomimetic Scaffolds for Tissue Engineering: 3D Printing Techniques in Regenerative Medicine - Frontiers." [Online]. Available: https://www.frontiersin.org/journals/bioengineering-and-biotechnology/articles/10.3389/fbioe.2020.586406/full

[16] "The promising applications of 3D printing technology in neurotrauma." [Online]. Available: https://www.accscience.com/journal/IJB/articles/online_first/1226

[17] "Mechanical Characterization of 3D-Printed Scaffolds: A Multi-Objective Optimization Approach Using Virtual Testing and Homogenization - MDPI." [Online]. Available: https://www.mdpi.com/2313-7673/10/9/580

[18] "Interactions of Cells and Biomaterials for Nerve Tissue Engineering: Polymers and Fabrication." [Online]. Available: https://pmc.ncbi.nlm.nih.gov/articles/PMC10536046/

[19] "Poly(lactide-co-glycolide) porous scaffolds for tissue engineering and regenerative medicine." [Online]. Available: https://pmc.ncbi.nlm.nih.gov/articles/PMC3363019/

[20] "Collagen for neural tissue engineering: Materials, strategies, and challenges - PMC." [Online]. Available: https://pmc.ncbi.nlm.nih.gov/articles/PMC10183670/

[21] "Chronic Imaging of Spinal Cord via Implantable Window in Rat Model - ResearchGate." [Online]. Available:

https://www.researchgate.net/publication/359909623_Chronic_Imaging_of_Spinal_Cord_via_Implantable_Window_in_Rat_Model

[22] "Printing splints with Dental LT Clear Resin - Support | Formlabs." [Online]. Available: https://support.formlabs.com/s/article/Printing-Splints-with-Dental-LT-Clear-Resin?language=en_US

[23] "US20190038273A1 - Surgical retractor - Google Patents." [Online]. Available: https://patents.google.com/patent/US20190038273A1/en

[24] "Linköping University Researchers Develop 'Skin in a Syringe' for 3D Printed Burn Grafts." [Online]. Available: https://3dprintingindustry.com/news/linkoping-university-researchers-develop-skin-in-a-syringe-for-3d-printed-burn-grafts-243084/

[25] W. Mirihanage *et al.*, "Structural Evolution of PCL during Melt Extrusion 3D Printing," *Macromol. Mater. Eng.*, pp. 1700494–1700500, 2018, doi: 10.1002/mame.201700494.

[26] "3D Printing of Scaffolds for Tissue Regeneration Applications - PMC." [Online]. Available: https://pmc.ncbi.nlm.nih.gov/articles/PMC4597933/

[27] "Acoustic and mechanical characterization of 3D printed scaffolds for tissue engineering applications | Request PDF - ResearchGate." [Online]. Available: https://www.researchgate.net/publication/326481433_Acoustic_and_mechanical_characterization_of_3D_printed_scaffolds_for_tissue_engineering_applications

[28] "Biocompatibility testing of tissue engineered products - ResearchGate." [Online].

Available:
https://www.researchgate.net/publication/8498098_Biocompatibility_testing_of_tissue_engineered_products

[29] "3D Bioprinting for Spinal Cord Injury Repair." [Online]. Available: https://pmc.ncbi.nlm.nih.gov/articles/PMC9065470/

[30] D. Popescu, C. Stochioiu, F. Baciu, and M. C. Iacob, "3D-Printed Polycaprolactone Mechanical Characterization and Suitability Assessment for Producing Wrist–Hand Orthoses. Polymers," vol. 15, no. 3. p. 576, 2023. doi: 10.3390/polym15030576.

[31] "Combination of Hyaluronic Acid Hydrogel Scaffold and PLGA Microspheres for Supporting Survival of Neural Stem Cells | Request PDF - ResearchGate." [Online]. Available: https://www.researchgate.net/publication/51093839_Combination_of_Hyaluronic_Acid_Hydrogel_Scaffold_and_PLGA_Microspheres_for_Supporting_Survival_of_Neural_Stem_Cells

[32] "Innovative Strategies in 3D Bioprinting for Spinal Cord Injury Repair - MDPI." [Online]. Available: https://www.mdpi.com/1422-0067/25/17/9592